Design of an undervoltage load shedding scheme for the Hydro-Québec system

Daniel Lefebvre

Hydro-Québec, Division TransEnergie
Complexes Desjardins, Tour de l'Est
CP 10000 Montreal (QC), Canada
lefebvre.daniel.4@hydro.qc.ca

Cédric Moors

Thierry Van Cutsem
Research Director, FNRS
University of Liège
Dept. of Elec. Eng. and Comp. Sc.
Sart Tilman B37 B-4000 Liège, Belgium
c.moors@ulg.ac.be t.vancutsem@ulg.ac.be

Abstract— **This paper deals with the control logic of an undervoltage, closed-loop load shedding scheme aimed at protecting the Hydro-Québec system against long-term voltage instability. This scheme relies on a set of "if-then" rules whose parameters are determined through combinatorial optimisation, relying on the system dynamic response over a set of scenarios. Preliminary results of the above optimisation technique are given, besides a brief description of the foreseen implementation.**

I. Introduction

There are two lines of defence against incidents likely to trigger system instability:

- *preventively*: estimate security margins with respect to credible contingencies, i.e. incidents with a relatively high probability of occurrence. Very often, preventive security criteria state that the system should respond in an acceptable way to (N-1)-type incidents, without the help of post-contingency actions affecting generators and/or loads;
- *correctively*: implement System Protection Schemes (SPS) (also referred to as Special Protection Schemes), to face the more severe, but less likely incidents. The latter are typically N-2 or more dangerous disturbances.

This paper focuses on corrective control of long-term voltage instability, driven by load tap changers, generator overexcitation limiters, switched shunt compensation, restorative loads, and possibly secondary voltage control [1], [2]. This type of instability has become a major threat in many systems.

While it should be used in the last resort, load shedding is an effective countermeasure against voltage instability [3], especially when the system undergoes a severe initial voltage drop that cannot be tolerated for a long time.

As for any SPS, the design of a load shedding scheme is a challenging task in terms of number of possible protection settings and (pre- and post-disturbance) scenarios to consider. Even study engineers with a very good knowlegde of their system face this huge complexity problem. Tools are thus needed to help them choosing the most appropriate designs.

This paper reports on the use of combinatorial optimisation for the tuning of a closed-loop load shedding controller aimed at protecting the Hydro-Québec system against long-term voltage instability. It is the continuation of the previous publications [4], [5], [6], considering a new controller structure, new criteria and new dimensioning scenarios.

II. Undervoltage load shedding in the Hydro-Québec system

With its long transmission corridors between the hydro generation areas in the North and the main load centers in the South part of the province (see Fig. 1), the Hydro-Québec (H-Q) system is exposed to angle, frequency and voltage stability problems.

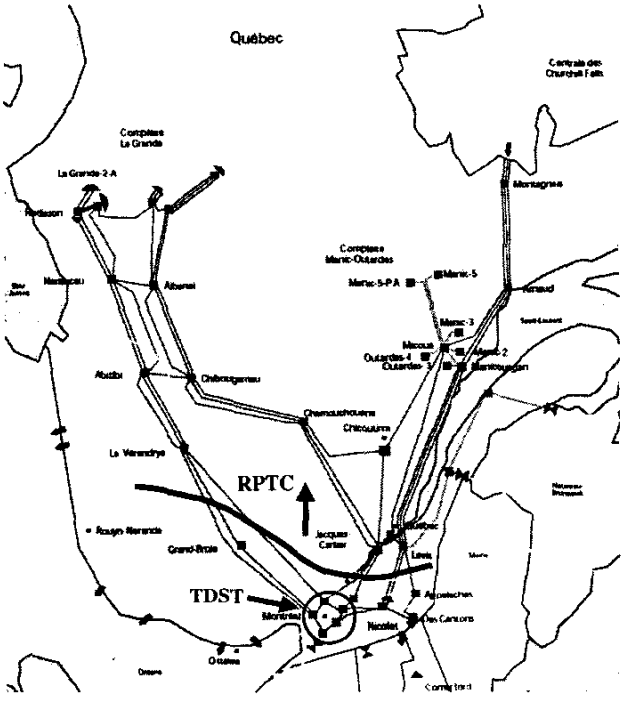

Fig. 1. Hydro-Québec EHV system with RPTC and TDST action zones

Besides static var compensators and synchronous condensers, the automatic shunt reactor switching devices - named

MAIS - play an important role in voltage control [7]. These devices, in operation since early 1997, are now available in twenty-two 735-kV substations and control a large part of the total 25,500 Mvar shunt compensation. Each MAIS device relies on the local voltage, the coordination between substations being performed through the switching delays. While fast-acting MAIS can improve transient angle stability, slower MAIS significantly contribute to voltage stability. MAIS devices react to voltage drops but also prevent overvoltages by reconnecting shunt reactors when needed.

In order to upgrade the reliability of its transmission system, H-Q has developed over the recent years an extensive defence plan against major disturbances. Besides traditional underfrequency load shedding measures, an extensive generation rejection and remote load shedding scheme - named RPTC - has been installed to face transient angle stability problems. The next step of this deployment is the undervoltage load shedding scheme - named TDST - whose implementation is scheduled for the beginning of 2004 (see Fig. 1).

While RPTC is an event-based SPS (due to the speed of angle instability phenomena), TDST will be *response-based* [8] (owing to the nature of long-term voltage instability), relying on transmission voltages measured in the Montreal area. More precisey, local voltages will be measured in five 735-kV substations equipped with MAIS devices and validated through the data acquisition chains of the latter. The measurement sampling rate will be 0.1 second. The average $\bar{V}$ of these local voltages will then be considered, provided that three valid values out of the five have been received.

The protection will rely on $\bar{V}$ not only to allow bad data rejection but also to better identify dangerous disturbances. Indeed, while an N-1 contingency (for which no load shedding is allowed) can affect one of the local voltages, it will have little effect on the average $\bar{V}$. Conversely, a significant drop of $\bar{V}$ is an indication that an N-2 or more severe disturbance has occured.

The shedding logic will rely on the absolute value of $\bar{V}$, as well as on the sudden decreases $\Delta\bar{V}$ of this signal. In normal operating conditions, the voltage profile of the H-Q system is maintaind in a narrow range around its nominal value (typically [0.98 1.02] pu) while the highest shedding threshold will be around 0.94 pu (a typical value of the critical voltage in this capacitive system). The $\Delta\bar{V}$ criterion is used to account for cases where pre-disturbance voltages would be at the upper limit of the above range. The voltage drop $\Delta\bar{V}$ is computed with respect to a reference V^o obtained by taking the average value of $\bar{V}$ over a sliding time window (of typically 30 s). As soon as $\bar{V}$ will drop by more 1%, the average value of $\bar{V}$ over the last available window will be taken as the reference V^o. Invalid values of $\bar{V}$ are discarded when computing V^o.

TDST will act in a pre-defined "load basin", of which it will be allowed to shed at most a certain percentage. The set of distribution circuit breakers that can be opened is known by the remote load shedding controller also used by RPTC.

By relying on $\bar{V}$, the protection is aimed at counteracting system-wide instability. In addition to this, local load shedding controllers will be attached to each of the five substations from which local voltage measurements are taken. Each of these controllers can act on a part of the above mentioned bassin. Their action will, however, be conditioned to some decrease of $\bar{V}$. These local controllers are not considered in the remaining of this paper.

III. The Undervoltage Load Shedding Logic

The control logic relies on the following:

3 rules, each allowed to act once:
R_1: *if* $\bar{V} < V_1^{min}$ *during* d_1 *seconds, shed* ΔP_1 *MW*
R_2: *if* $\bar{V} < V_2^{min}$ *during* d_2 *seconds, shed* ΔP_2 *MW*
R_3: *if* $\bar{V} < V_3^{min}$ *during* d_3 *seconds, shed* ΔP_3 *MW*
1 rule allowed to act several times, provided that (at least) one of the above has been already activated:
R_I: *if* $\bar{V} < V_I^{min}$ *during* d_I *seconds, shed* ΔP_I *MW, where the larger* $V_I^{min} - \bar{V}$*, the larger* ΔP_I

Rules R_1 to R_3 aim at making the voltage promptly recover once it has dropped below an unacceptable level (e.g. from the customer viewpoint). The V_1^{min} parameter is set at this level, while the other voltage thresholds are such that :

$$V_3^{min} < V_2^{min} < V_1^{min} \tag{1}$$

Each rule corresponds to a different level of severity. Correspondingly, the load shedding amounts and delays are chosen so that the deeper the voltage drop, the larger the shedding:

$$\Delta P_3 > \Delta P_2 > \Delta P_1 \tag{2}$$

and the shorter the delay:

$$d_3 < d_2 < d_1 \tag{3}$$

Alternative choices may be thought of. For instance, there might be less or more rules, although in the latter case, the computational effort of the optimisation should be kept in mind. Also, the inequalities (2, 3) are not mandatory, although they have been found to work well.

The idea behind rule R_I is to set up a controller adjusting its action to the severity of the situation. The latter is assessed through the average voltage drop over the time interval d_I. To this purpose, the load shedding step is given by:

$$\Delta P_I = k\,\Delta\bar{V}_{avg} \quad \text{with} \quad \Delta P_I^{min} \leq \Delta P_I \leq \Delta P_I^{max} \tag{4}$$

where $\Delta\bar{V}_{avg}$ is the average voltage drop :

$$\Delta\bar{V}_{avg} = \frac{1}{d_I}\int_{t_0}^{t_0+d_I} (V_I^{min} - \bar{V})dt \tag{5}$$

and t_o is the time at which $\bar{V}$ falls below V_I^{min}. Clearly, the larger $V_I^{min} - \bar{V}$, the larger ΔP_I.

Finally, ΔP_I is discretized as indicated in Fig. 2, to take into account that loads are shed by blocks (when opening circuit breakers).

While the main purpose of R_1, R_2, R_3 is to react to a severe voltage drop, the role of R_I is the final stabilization of the

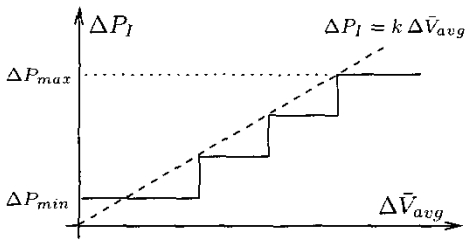

Fig. 2. Discretization of load shedding

system. In this respect, the thresholds of R_1 and R_I are such that:

$$V_1^{min} < V_I^{min} \tag{6}$$

With V_I^{min} set to a higher value, the risk increases of an undue load shedding following a large system transient. On the basis of simulations, it is possible to tune the protection parameters to avoid such false alarms; however, the uncertainty affecting the simulation models must be considered as well. Therefore, to increase the protection security, H-Q has decided to condition the application of R_I to the previous triggering of (at least) one of the rules R_1 to R_3.

Rules R_1, R_2, R_3 are "concurrent" in the sense that any of them can be applied irrespective of the others. However, each rule may be triggered only once.

On the other hand, R_I is conditioned to the other rules, as explained above, but can be applied repetitively. This yields a *closed-loop* design since the protection may act several times, each action being based on the measured result of the previously taken actions, and adjusted in amplitude to the system evolution. This closed-loop design guarantees a higher SPS robustness against modelling uncertainties at the design stage.

Note finally that by adjusting its action to the severity of the situation, the controller minimizes the risk of overfrequency (and thermal unit tripping) due to excessive load shedding.

IV. Optimisation of the Load Shedding Controller

The methodology used to adjust the settings of TDST consists of two steps [6]. In the first step, a set of training scenarios is built, and each unstable scenario of this set is analyzed to determine the minimal load shedding needed. In the second step, the protection parameters are adjusted in order to approach as closely as possible the optimal sheddings computed in the first step, over the whole set of scenarios. A combinatorial optimization method is used to this purpose.

A. Scenario analysis

The first step thus consists in setting up a set of s training scenarios, corresponding to various topologies, load levels, generation schemes, contingencies, etc. Given the load basin that TDST will control, for each scenario, we determine $P_i^\star \quad (i = 1, ..., s)$, the minimal amount of load to shed *at a single point in time*.

To this purpose, for a given shedding delay τ, the minimal amount P_i^{min} of load to shed is determined iteratively by incremental or binary search [6]. This determination is repeated for various values of τ; $P_i^\star$ is then taken as the minimum of the $P_i^{min}(\tau)$ curve.

An example of such a curve is given in Fig. 3 for the Hydro-Québec system. For the scenario of concern, the best time to shed load is 15 to 20 seconds (or 35 to 40) seconds after the disturbance. This delay allows the MAIS to trip shunt reactors and hence to increase the network transmission capability, thereby reducing the amount of load to shed. Shedding earlier resets the MAIS by increasing the transmission voltages monitored by these devices. The value of $P_i^\star$ is 650 MW.

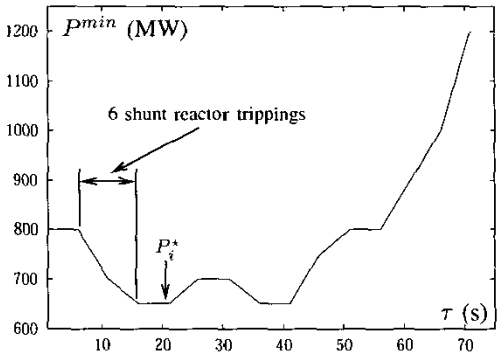

Fig. 3. minimal load shedding vs. shedding delay in a given scenario

B. Statement of the optimization problem

Let us denote by $\mathbf{x}$ the vector of all parameters which appear in the rules and hence have to be adjusted:

$$\begin{aligned}\mathbf{x} \;=\; & [\Delta P_1\ \Delta P_2\ \Delta P_3\ d_1\ d_2\ d_3\ V_2^{min}\ V_3^{min} \\ & k\ \Delta P_I^{min}\ \Delta P_I^{max}\ V_I^{min}\ d_I]\end{aligned} \tag{7}$$

Given the s training scenarios, the problem is to determine $\mathbf{x}$ such that the following requirements are met:

1) the amount of load shedding must be as close as possible to the ideal value $P_i^\star$ determined in the first step;
2) all unstable scenarios must be saved (dependability);
3) no load must be shed in a stable scenario (security);
4) the average voltage $\bar{V}$ must not stay below V_1^{min} for more than some time.

This can be translated into an optimization problem: minimize either the L_1 objective:

$$\frac{1}{s}\sum_{i=1}^{s}\left[P_i^{sh}(\mathbf{x}) - P_i^\star + p_i(\mathbf{x})\right] \tag{8}$$

or the L_∞ objective:

$$\max_i\left[P_i^{sh}(\mathbf{x}) - P_i^\star + p_i(\mathbf{x})\right] \tag{9}$$

where, in the i-th scenario, $P_i^{sh}(\mathbf{x})$ is the total load power shed by the controller and $p_i(\mathbf{x})$ is a penalty term accounting

for the violation of the above requirements. In Eq. (8) (resp. (9)), the sum (resp. the max) extends over the unstable scenarios. The expression within brackets is expected to be positive since:

- $P_i^{sh}(\mathbf{x}) > P_i^{\star}$: indeed, more load has to be dropped when shedding in several steps (as the controller does) rather than a single one (as assumed when computing $P_i^{\star}$). This assertion has been verified in all our simulations;
- $p_i(\mathbf{x}) \geq 0$. For details about the choice of the penalties, please refer to [5], [6].

C. The Branch-and-Bound approach

The above optimization problem is complex. Indeed, both P_i^{sh} and p_i must be determined from time-domain simulations and hence, explicit analytical expressions cannot be established. Moreover, they vary with $\mathbf{x}$ in a discontinuous manner, which prevents from using mathematical programming methods. Finally, multiple local minima are expected. This is why we prefer to resort to combinatorial optimization.

To this purpose, each component of $\mathbf{x}$ is discretized in a finite number of possible values. The discretization steps are chosen in accordance with the engineering knowledge of the problem (see Section V.A).

Evaluating the L_1 or L_∞ objectives for a given protection setting requires to simulate the s scenarios (in order to compute the s terms $P_i^{sh}(\mathbf{x}) - P_i^{\star} + p_i(\mathbf{x})$). This time-consuming step precludes a brute-force enumeration of all the discrete instances of $\mathbf{x}$.

Luckily, a short-cut can dramatically decrease the computational effort. It consists, during the enumeration of the various instances of $\mathbf{x}$, in keeping track of I_b, the best value of the objective obtained so far. I_b is an upper bound on the sought global minimum. Now, as the various scenarios are being checked for a given instance of $\mathbf{x}$, the objective function can only increase. Therefore, as soon as the objective function becomes greater than I_b, the scenario enumeration can be broken and the current instance of $\mathbf{x}$ abandoned; otherwise, the value of the objective becomes the new I_b. This procedure is outlined in Fig. 4, where $\mathbf{x}^{(j)}$ denotes the j-th instance of $\mathbf{x}$ $(j = 1, \ldots, N)$.

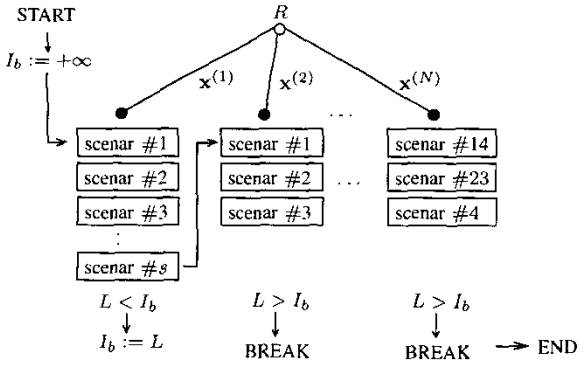

Fig. 4. sketch of the Branch-and-Bound method

This significant short-cut of the enumerative search is nothing but an application of the *Branch-and-Bound* principle [9]. Note that when the load shedding controller only involves rules of the type R_1, R_2, R_3, the optimization problem can be formulated as a tree exploration and an improved bound can be built, from which further speed-up can be obtained with the Branch-and-Bound method [6].

When using the L_1 objective, the gain in computing time is expected to be smaller. Indeed, due to the additive nature of this objective, a higher number of scenarios have usually to be simulated before the objective function reaches the I_b value. This is a drawback of the L_1 objective. On the other hand, this objective usually behaves more smoothly, i.e. is less sensitive to small changes in parameters [6].

It is easily seen from the above description that the performance will be improved if I_b decreases at an early stage of the search and/or the scenarios with the largest contribution to the objective are processed first. As regards the second aspect, it may be advantageous to *dynamically reorder the scenarios* on the basis of their ability to break enumerations, observed at the beginning of the search or in previous optimizations [6].

D. Distributed processing

In spite of the effectiveness of the Branch-and-Bound algorithm, the computational burden may remain prohibitive, especially when the L_1 objective is considered or when the size of the search space to explore is important. Fortunately, the very structure of the problem makes it easy to distribute computations on several "slave" processors coordinated by a "master" one.

In the *first scheme* to come to mind the master assigns the simulation of a scenario to each slave (as soon as it becomes available) and receives from the latter the value of P_i^{sh} and the stable/unstable diagnosis. Enumeration breaks and I_b updates are taken care of by the master. This scheme is efficient in so far as the time for transferring the data from the master to a slave is small compared to the simulation time, so that the communication overhead remains negligible.

An alternative consists of using each slave to explore a subset of instances of $\mathbf{x}$. In this *second scheme*, as soon as I_b decreases, the new value must be broadcasted to all the other slaves.

E. Time simulation tools

Detailed long-term voltage instability simulations remain time consuming. This computational burden does not exist with the Quasi Steady-State (QSS) simulation, a well-documented simplified long-term simulation technique [2].

QSS simulation is useful for processing a large search space and taking preliminary decisions, for instance deciding which parameters will be subsequently fixed, to save computing time.

An example of comparison between QSS and detailed simulations is given in Fig. 5, in an unstable case without load shedding. As can be seen, the long-term behaviour is well captured by the QSS simulation but, expectedly, the short-term transients (taking place over the first 20 seconds) are not

reproduced. This period of time where voltage and frequency experience large transients has to be simulated in detail in order to properly set the protection parameters.

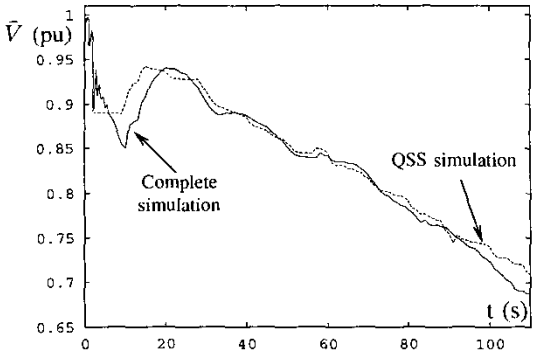

Fig. 5. QSS vs. detailed simulation (unstable case)

In this respect, the coupling between full and QSS simulations presented in [10] is a very interesting compromize between efficiency and accuracy. The idea is to simulate the short-term period using detailed simulation and, once the transients have died out, to switch to QSS simulation, the latter being initialized "out of equilibrium".

V. Results

A. Training scenarios and criteria

The study reported in this paper involves 22 system configurations, summarized in Table I.

TABLE I
SYSTEM CONFIGURATIONS CONSIDERED IN THE TRAINING SCENARIOS

configuration	number of 735-kV lines out of service	number of synchronous condensers	number of MAIS devices	load active power exponent
A	0	6	6	1
B	1	6	6	1
C	1	8	6	1
D	1	8	6	1
E	1	7	4	1
F	1	8	10	1
G	1	7	6	1
H	4	8	6	1
I	4	7	4	1
J	3	8	10	1
K	3	7	6	1
L	3	8	10	1
M	3	7	6	1
N	1	7	3	1
O	1	7	4	1
P	1	7	4	1
Q	3	7	5	1
R	0	6	6	1.3
S	1	8	6	1.3
T	1	8	6	1.3
U	4	8	6	1.3
V	3	7	6	1.3

Table II details the 38 scenarios finally selected. They involve N-1, N-2 and N-3 contingencies, respectively. In accordance with the standard operating rules, the system is stable following any N-1 incident. The MAIS devices can be used to this purpose.

TABLE II
DESCRIPTION OF THE 38 TRAINING SCENARIOS

No	conf.	incid. type	$P_i^\star$ (MW)	No	conf.	incid. type	$P_i^\star$ (MW)
1	A	N-1	0	20	G	N-2	300
2	A	N-1	0	21	O	N-2	100
3	R	N-2	650	22	P	N-2	300
4	A	N-2	400	23	H	N-1	0
5	R	N-3	1100	24	H	N-1	0
6	B	N-1	0	25	I	N-2	300
7	B	N-2	400	26	U	N-2	1450
8	C	N-1	0	27	H	N-2	1200
9	C	N-2	200	28	U	N-2	650
10	S	N-2	1250	29	J	N-1	0
11	C	N-2	550	30	J	N-1	0
12	D	N-1	0	31	K	N-2	300
13	D	N-1	0	32	J	N-2	800
14	E	N-2	150	33	V	N-2	600
15	N	N-2	300	34	L	N-1	0
16	T	N-2	850	35	L	N-1	0
17	D	N-2	750	36	Q	N-2	0
18	F	N-1	0	37	M	N-2	500
19	G	N-2	0	38	Q	N-2	0

The training set includes 16 stable scenarios in order to train the protection not to act in stable cases. In the 22 unstable scenarios, the minimal load shedding $P_i^\star$ has been determined as outlined in Section IV-A. The values, computed with an accuracy of 50 MW, are given in Table II. In this study, load shedding is shared out between 10 locations, each load being decreased proportionally to its initial value. As can be seen from Table II, the $P_i^\star$ values range rather uniformly in the [100 1450] MW interval, between marginally and severely unstable cases.

Requirements 1 to 4 of Section IV-B have been taken into account. In accordance with Hydro-Québec planning rules, the 3rd requirement has been amended by allowing some (hopefully small) load shedding to take place after a stable but severe incident. The N-2 scenario No 19 is concerned. The latter is handled as an unstable scenario with $P_i^\star = 0$ in (8) and (9). This leads to finally processing $s = 22 + 1 = 23$ scenarios. As regards the 4th requirement, the average voltage $\bar{V}$ is not allowed to stay below $V_1^{min} = 0.94$ pu for more than 15 seconds.

B. Search spaces

Tables III and IV detail the two search spaces considered in this study, referred to as SP1 and SP2, respectively. The main difference between them concerns the number of unknowns to determine. In SP1, the parameters of rules R_1, R_2 and R_3 are fixed to values suggested by preliminary trial-and-error simulations. Hence, the parameters to be optimized (indicated with bold font) are those associated with the R_I rule.

On the other hand, the purpose of SP2 is to let the methodology find the best parameters of rules R_1, R_2 and R_3 as well. The exponential complexity of the combinatorial optimization makes it nonetheless necessary to limit the number

TABLE III

SEARCH SPACE 1

Rule	Param.	Lower bound	Upper bound	Nb. of values
R_1	V_1^{min} (pu)		0.94	
	d_1 (s)		11	
	ΔP_1 (MW)		400	
R_2	V_2^{min} (pu)		0.93	
	d_2 (s)		9	
	ΔP_2 (MW)		400	
R_3	V_3^{min} (pu)		0.91	
	d_3 (s)		6	
	ΔP_3 (MW)		700	
R_I	$\mathbf{V_I^{min}}$ (pu)	0.94	0.95	2
	$\mathbf{d_I}$ (s)	3	8	6
	$\mathbf{k}$ (MW/pu)	5000	15000	11
	$\mathbf{\Delta P_{min}}$ (MW)	0	400	5
	$\mathbf{\Delta P_{max}}$ (MW)	100	1000	10
Total number of instances of $\mathbf{x}$			5280	

TABLE IV

SEARCH SPACE 2

Rule	Param.	Lower bound	Upper bound	Nb. of values
R_1	V_1^{min} (pu)		0.94	
	$\mathbf{d_1}$ (s)	10	14	5
	$\mathbf{\Delta P_1}$ (MW)	100	400	4
R_2	V_2^{min} (pu)		0.92	
	d_2 (s)		$d_1 - 4$	
	$\mathbf{\Delta P_2}$ (MW)	200	500	4
R_3	V_3^{min} (pu)		0.9	
	d_3 (s)		$d_1 - 8$	
	$\mathbf{\Delta P_3}$ (MW)	600	900	4
R_I	V_I^{min} (pu)		0.95	
	$\mathbf{d_I}$ (s)	3	8	6
	$\mathbf{k}$ (MW/pu)	7000	15000	9
	$\mathbf{\Delta P_{min}}$ (MW)	0	300	4
	$\mathbf{\Delta P_{max}}$ (MW)	400	600	3
Total number of instances of $\mathbf{x}$			77760	

of unknowns as well as the values tested for each of them. In this respect, the thresholds V_2^{min} and V_3^{min} have been chosen from the observation of the very first voltage drops (after the disturbance occurrence). They have also been chosen to that each rule is optimized from a significant number of scenarios. Finally, the size of the search space has been further reduced by "linking" the delays d_1, d_2 and d_3 as indicated in Table IV.

The total number of instances of $\mathbf{x}$ is given in both tables. The only considered designs are those satisfying inequalities (2), (3) and (4). Taking into account that each combination has to be tested over 23 scenarios, these figures confirm the huge complexity of the combinatorial optimization.

C. Computing tools

As of writing this paper, tests with detailed simulation are under progress. Therefore, we present hereafter the results of a preliminary study using QSS simulation.

To speed up computations, the dynamic reordering technique mentioned in Section IV-C has been used.

Finally, when optimizing the L_1 objective from SP2, the computations have been distributed over 4 PCs, according to the second scheme of section IV-D

D. Results and discussion

Table V shows, for each search space and each objective, the optimal value found for the various parameters and the value of the corresponding objective. For information only, the value of the other (non optimized) objective is given in parentheses underneath the first one. Let us emphasize that all four requirements of Section IV-B are met in all designs of Table V.

TABLE V

OPTIMIZATION RESULTS

Param.	SP1		SP2	
	L_∞	L_1	L_∞	L_1
V_1^{min} (pu)	0.94	0.94	0.94	0.94
d_1 (s)	11	11	10	10
ΔP_1 (MW)	400	400	100	100
V_2^{min} (pu)	0.93	0.93	0.92	0.92
d_2 (s)	9	9	6	6
ΔP_2 (MW)	400	400	200	200
V_3^{min} (pu)	0.91	0.91	0.9	0.9
d_3 (s)	6	6	2	2
ΔP_3 (MW)	700	700	600	600
V_I^{min} (pu)	0.94	0.95	0.95	0.95
d_I (s)	3	3	3	3
k (MW/pu)	15000	11000	7000	7000
ΔP_{min} (MW)	300	100	300	200
ΔP_{max} (MW)	400	400	400	400
Objective value	400 (196)	167 (600)	400 (170)	148 (600)

As can be seen, the performances of the controllers found from the two search spaces are the same when the L_∞ objective is considered (see 2nd and 4th columns of the table). On the other hand, optimizing the L_1 objective from SP2 allows to find a better design (see 3rd and 5th columns). This result indicates that, while the primary objective of rules R_1 to R_3 is to make voltages promptly recover, they are also useful to improve the controller performances in terms of shed amounts. The final choice between the two objectives will be made from the results of detailed simulations.

Figures 6 and 7 show two typical time evolutions of $\bar{V}$ for one of the obtained designs.

In Fig. 6, the behaviour is typical of a "traditional" under-voltage load shedding scheme. In the first seconds following the occurrence of the disturbance, several rules are activated to shed an important amount of load, in order $\bar{V}$ to be brought back above 0.94 pu. The final stabilization is then guaranteed by MAIS devices and the R_I rule.

The situation is different in Fig. 7: although $\bar{V}$ falls below V_1^{min} and V_2^{min} just after the disturbance, the controller takes advantage of the MAIS devices, which make $\bar{V}$ recover above 0.94 pu. Once the voltage decrease resumes, the controller has to wait for rule R_1 to shed 400 MW; then, it relies on rule R_I to adjust its action to the severity of the situation. This allows the total load shed (700 MW) to be very close to the target value ($P_i^\star$ = 650 MW).

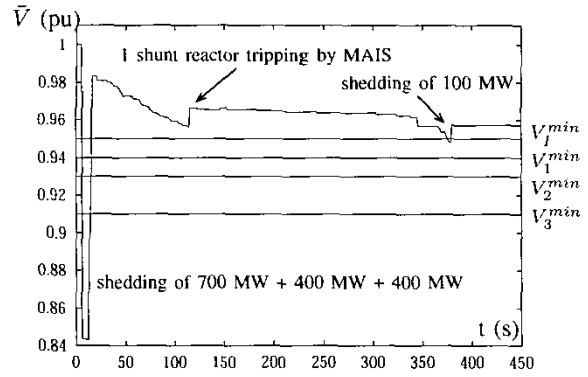

Fig. 6. Time evolution of $\bar{V}$ in scenario 26

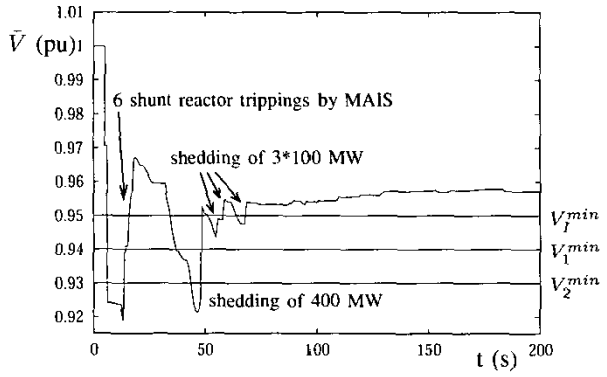

Fig. 7. Time evolution of $\bar{V}$ in scenario 28

Table VI compares the total number of simulations required to design the controller from the two search spaces. These figures confirm that optimizing the L_1 objective requires more simulations and hence is more time consuming. The gain with respect to a brute force enumeration is much more important in the case of L_∞, as discussed in [6].

However, the optimization of L_1 from SP2 shows an interesting result: sharing out the search space between several processors (which was not done for SP1) allows to break more enumerations and hence reject a larger percentage of (useless) designs. Indeed, with 4 processors working in parallel, lower values of I_b have been discovered sooner, and broadcasted to the other processors. From the computing time viewpoint, this adds to the gain naturally obtained from parallel computations. These two speed-ups cumulated bring an overall gain in computing time of 15.

VI. Conclusion

This paper has described some characteristics of TDST, an undervoltage load shedding scheme scheduled for implementation in the Hydro-Québec system by the beginning of 2004. The emphasis was on the control logic. Obviously, many other practical aspects, essential for the reliability of such a system protection scheme, have not been considered here.

TABLE VI

TOTAL NUMBER OF SIMULATIONS REQUIRED FOR THE OPTIMIZATIONS

	SP1		SP2	
	L_∞	L_1	L_∞	L_1
Brute force enumeration	121440	121440	1788480	1788480
B&B approach	7773	101322	98242	331479
Gain	16	1.2	18	5.4

TDST will rely on four *if-then rules*. Three of them aim at making the average voltage promptly recover above some admissible level, and will make up the first line of defence against voltage instability. Conditioned to the previous triggering of these rules, the fourth one is allowed to act several times and to adjust its action to the severity of the situation, thereby yielding a robust closed-loop protection.

The combinatorial optimization (Branch-and-Bound) methodology previously proposed by the authors to optimize the parameters of the above rules, has been applied to this new structure, using a new set of dimensioning scenarios. The results of a preliminary study have been presented in this paper. Tests with detailed simulations are under progress. Distributed processing, as outlined in this paper, is essential to keep the optimization approach tractable while investigating a sufficiently large search space for the protection parameters.

Obviously, the final tuning of TDST will have to take into account several other aspects, such as the coordination with the existing RPTC.

The method is already useful to assist Hydro-Québec engineers in the highly combinatorial and multi-faceted task of adjusting TDST parameters. It will also prove useful for updating the protection parameters, for instance when transmission system reinforcements will come into effect.

References

[1] C. W. Taylor, Power System Voltage Stability, McGraw Hill, EPRI Power System Engineering series, 1994

[2] T. Van Cutsem, C. Vournas, Voltage Stability of Electric Power Systems, Boston, Kluwer Academic Publishers, 1998

[3] C. W. Taylor, "Concepts of undervoltage load shedding for voltage stability", IEEE Trans. on Power Delivery, Vol. 7, pp. 480-488, 1992

[4] C. Moors, D. Lefebvre, T. Van Cutsem, "Load Shedding Controllers Against Voltage Instability: a Comparison of Designs", Proc. of the IEEE Power Tech Conference, Porto (Portugal), 2001, ISBN 0-7803-7140-2

[5] C. Moors, D. Lefebvre, T. Van Cutsem, "Design of load shedding schemes against voltage instability", IEEE Power Engineering Society Winter Meeting, Singapore, 2000

[6] C. Moors, On the Design of Load Shedding Schemes against Voltage Instability in Electric Power Systems, PhD thesis, University of Liège, Fac. of Applied Sciences, October 2002

[7] S. Bernard, G. Trudel, G. Scott, "A 735-kV shunt reactors automatic switching system for Hydro-Québec network", IEEE Trans. on Power Systems, Vol. 11, pp. 2024-2030, 1996

[8] CIGRE Working Group 34-02-19, System Protection Schemes in Power Networks, CIGRE publication, 2001

[9] W. S. Cook, W. H. Cunningham, W. R. Pulley Blank, A. Schrijver, Combinatorial Optimization, Wiley-Interscience, 1998

[10] L. Loud, P. Rousseaux, D. Lefebvre, T. Van Cutsem, "A time-scale decomposition-based simulation tool for voltage stability analysis", Proc. of the IEEE Power Tech Conference, Porto (Portugal), 2001, ISBN 0-7803-7140-2.